

# Performance Analysis of Multiuser Detection for Multibeam Satellites Under Rain Fading

Jesús Arnau and Carlos Mosquera  
Signal Theory and Communications Department  
University of Vigo - 36310 Vigo, Spain  
{susos, mosquera}@gts.uvigo.es

**Abstract**—Multibeam satellite systems are nowadays widely employed, and their use is expected to grow in the next decades. This has raised the interest for signal processing techniques able to mitigate the interference among beams, since they could enable a much more aggressive spectrum reuse. From an engineering point of view, the system design must consider as an option aggressive frequency reuse patterns, with the need to evaluate the performance of the corresponding interfering canceling techniques for the usual impairments and non-idealities of the satellite link. In this paper, we investigate the effect of a practical impairment of great importance, namely, the attenuation due to the rain, on the performance of a return link which performs MMSE interference canceling. Analytical expressions are derived for a number of performance measures based on the statistical characterization of the rain attenuation.

**Index Terms**—Multiuser detection; on-ground beamforming; rain fading; multibeam satellites.

## I. INTRODUCTION

In the last few years, the use of multiple spot beams in modern broadband satellites has increased, in an effort to serve higher throughput demands with a scalable cost. For this task, frequency reuse among users beams is required and, if total spectrum reuse is the goal, then it is necessary to somehow counteract the interference among beams that appears due to the side lobes in the satellite's radiation pattern.

Recently, many studies such as [1], [2], [3] have been conducted in order to evaluate the performance of interference mitigation techniques. As shown in these references, the trend is to shift the complexity of the extra processing needed to the Earth segment, by relaying the whole set of received signals to the gateway station. More specifically, the performance of the return link of such a full on-ground architecture was investigated in [4], featuring an adaptive coding and modulation (ACM) enhanced DVB-RCS physical layer. Results showed an increase in throughput at the cost of some loss in availability.

From an information theoretic point of view, the return link corresponds to a multiple access channel (MAC) [5]. Its maximum sum rate is known to be achieved via successive

interference cancellation with minimum mean-squared error filtering at each stage (MMSE-SIC) [6]. However, much simpler, linear alternatives, such as the zero-forcing (ZF) receiver or the plain linear MMSE receiver (LMMSE) ([7], [8]) are also popular because of their lower computational complexity.

However, the use of these techniques demands new system design strategies that predict their performance, under a number of practical impairments, and make design decisions accordingly. One of the most important impairments, specially in bands such as the Ka band and above, is the attenuation induced by the presence of rain in the link.

In this paper, we will focus on studying the performance of a return link impaired by rain fading. It will be shown that the achievable sum rate tends to suffer a constant loss as the SNR increases, and that such loss can be computed in closed form from the parameters of the rain fading distribution. Moreover, an expression for the probability of outage of the instantaneous capacity will be derived, and the behavior of a given user's SINR after interference canceling will be additionally studied, showing that it results in a scaling of its original value by a rain-dependent variable; all these results will be tested by detailed computer simulations.

The remainder of the paper is structured as follows: Section II describes the system model and the performance metrics that will be studied, Section III derives expressions for the system MSE and the performance of a single user in terms of SINR, Section IV presents analytical expressions for the maximum sum rate of the system under rain fading, Section V reports the results obtained by computer simulations and, finally, conclusions are drawn on Section VI.

## II. SYSTEM MODEL AND PERFORMANCE METRICS

### A. Model under Study

The object of study consists of a single satellite which gives service to a region covered by  $K$  beam spots; a single user link is active at a given time and carrier block at each beam. The satellite uses a fed reflector antenna array with  $N$  ( $N \geq K$ ) feeds to exchange signals with the user terminals (UT). All these signals will be relayed through a feeder link to the gateway station (GW) on Earth. In the sequel, we will assume a single gateway and neglect the possible impairments caused by the feeder link.

Research funded in part by the European Space Agency under ESTEC Contract No. 23089/10/NL/CLP, ESA Support to the SatNEx III Network of Experts, and by the European Regional Development Fund (ERDF) and the Spanish Government under projects DYNACS (TEC2010-21245-C02-02/TCM) and COMONSENS (CONSOLIDER-INGENIO 2010 CSD2008-00010), and the Galician Regional Government under projects Consolidation of Research Units 2009/62 and 2010/85.

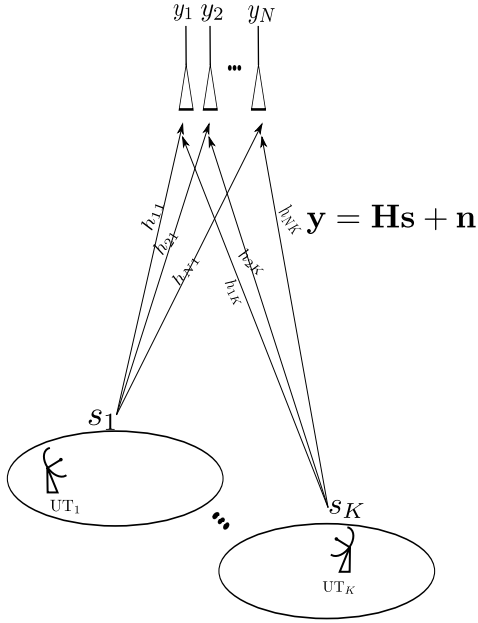


Figure 1. Descriptive graphic of the system model assumed.

The mathematical model of the return link reads

$$\mathbf{y} = \mathbf{H}\mathbf{s} + \mathbf{n} \quad (1)$$

where  $\mathbf{y}$  is an  $N \times 1$  vector that contains the symbols received at each feed,  $\mathbf{s}$  is a  $K \times 1$  stack of the symbols transmitted by each user,  $\mathbf{n}$  is the  $N \times 1$  vector of zero-mean complex white Gaussian noise samples, such that  $\mathbb{E}[\mathbf{n}\mathbf{n}^H] = N_0 \cdot \mathbf{\Sigma}$ , and  $\mathbf{H}$  represents the  $N \times K$  channel matrix (see Fig. 1 for a graphical description). The channel flat-frequency response is parameterized as

$$\mathbf{H} = \sqrt{P} \cdot \mathbf{G}\mathbf{A} \quad (2)$$

where  $P$  is the transmit power, which we will assume equal for all users, and each matrix is described in the following paragraphs.

1) *Feed Radiation Pattern and Path Losses*:  $\mathbf{G}$  is assumed to be an  $N \times K$  matrix that accounts for the gains of the feed radiation pattern, the on-board attenuation and the free space losses; recall that the feeder link is considered transparent. Matrix  $\mathbf{G}$  can be considered deterministic upon the assumption of fixed stations on Earth.

2) *Atmospheric Fading*: The attenuation due to atmospheric phenomena can be significant in bands such as the Ka-band. In this study, we will focus on the effect of rain fading upon the performance of our system. To do so, we use the common assumption (see for instance [9]) that rain attenuation, in dB, can be modeled following a log-normal distribution, as specified in Recommendation ITU-R P.1853; let  $L_i$  be the power loss suffered by the  $i$ -th user, in dB, then  $L_i \sim \mathcal{LN}(\mu_i, \sigma_i^2)$ , where  $\mu_i$  is the log-normal *location parameter* and  $\sigma_i$  the *shape parameter*. Consequently, the corresponding amplitude attenuation value in natural units will be expressed as

$$l_i = 10^{-\frac{L_i}{20}} \quad (3)$$

and the associated complex fading coefficient as

$$a_i = l_i e^{j\phi_i} \quad (4)$$

where  $\phi_i$  represents random fluctuations in the phase; in this study, its behavior will be left unexplained because, as we will show, it will have no effect on the performance metrics considered.

Following the considerations above, matrix  $\mathbf{A}$  can be expressed as

$$\begin{aligned} \mathbf{A} &= \begin{pmatrix} l_1 & 0 & \cdots & 0 \\ 0 & l_2 & \cdots & 0 \\ \vdots & \vdots & \ddots & \vdots \\ 0 & 0 & \cdots & l_K \end{pmatrix} \begin{pmatrix} e^{j\phi_1} & 0 & \cdots & 0 \\ 0 & e^{j\phi_2} & \cdots & 0 \\ \vdots & \vdots & \ddots & \vdots \\ 0 & 0 & \cdots & e^{j\phi_K} \end{pmatrix} \\ &= \mathbf{L}\mathbf{\Phi} \end{aligned} \quad (5)$$

Firstly, it is important to notice that  $\mathbf{A}^H \mathbf{A} = \mathbf{A}\mathbf{A}^H = \mathbf{L}^2$ . Secondly, through all the work we will be assuming that the different  $l_i$  are independent, that is, that the spatial correlation among the rain attenuation experimented by the different beams is negligible. As explained in [10], this correlation decreases fast with the beam radius, so that it can be neglected for most beam sizes of practical interest; as an example, in [9] the correlation is treated as zero for a beam diameter of 250 km.

## B. Performance Metrics

1) *Maximum Sum Rate*: Recall that, from an information theoretic point of view, the satellite RL is a MAC channel and, thus, the achievable sum rate is upper bounded by the expression of the *ergodic capacity*, that is [11],

$$\sum_{i=1}^K R_k \leq C = \mathbb{E} \left[ \log_2 \det \left( \mathbf{I} + \frac{1}{N_0} \mathbf{H}\mathbf{\Sigma}^{-1} \mathbf{H}^H \right) \right] \quad (6)$$

where we are assuming full Channel State Information (CSI) at the receiver. Throughout this paper,  $C$  will be referred to as the *maximum sum rate*, while its value before performing the expectation, i.e.,  $\log_2 \det \left( \mathbf{I} + \frac{1}{N_0} \mathbf{H}\mathbf{\Sigma}^{-1} \mathbf{H}^H \right)$  will be called *instantaneous capacity*.

The interest of this metric relies on the fact that it provides an upper bound to the achievable performance. Moreover, the MMSE-SIC receiver is known to achieve the maximum sum rate in an ideal case [6] and, as it will be shown, insights on the spectral efficiency of much simpler receivers can be derived from it also.

2) *Mean Squared Error after LMMSE*: One of the main drawbacks of the MMSE-SIC combiner is its complexity, which may render it unusable in systems with a large number of users. Among the remaining interference mitigation techniques, the plain LMMSE receiver is one of the most popular ones, partly because of its optimum balance between noise suppression and interference cancellation, and also because of its relatively low computational complexity. Its expression is

as follows: from the received vector  $\mathbf{y}$ , the transmitted symbols would be obtained as  $\hat{\mathbf{x}} = \mathbf{W}^H \mathbf{y}$  with [7]

$$\mathbf{W}^H = (\mathbf{I} + \mathbf{H}^H \boldsymbol{\Sigma}^{-1} \mathbf{H})^{-1} \mathbf{H}^H \boldsymbol{\Sigma}^{-1}. \quad (7)$$

We will be interested in studying the mean-squared error (MSE) after combining, which is defined as  $\mathbb{E}\{|\mathbf{x} - \hat{\mathbf{x}}|^2\}$ . Its covariance matrix, denoted as  $\mathbf{Q}$ , would read as

$$\mathbf{Q} = \mathbf{R}_s - \mathbf{R}_{sy} \mathbf{R}_y^{-1} \mathbf{R}_{ys} = \left( \mathbf{I} + \frac{1}{N_0} \mathbf{H}^H \boldsymbol{\Sigma}^{-1} \mathbf{H} \right)^{-1} \quad (8)$$

where the error for the  $i$ -th user would be expressed as

$$\epsilon_i^2 = \mathbf{Q}_{ii} \quad (9)$$

so that, averaging over all the users, the following expression is obtained

$$\epsilon^2 = \frac{1}{K} \text{trace } \mathbf{Q}. \quad (10)$$

3) *SINR after LMMSE*: For the case of the LMMSE receiver, it is possible to go even further and derive the expression of a specific user SINR after performing this processing. In fact, one of the main interests for studying the MSE metric is that its expression is closely related to that of the SINR:

$$\begin{aligned} \rho_i &= \frac{1}{\epsilon_i^2} - 1 \\ &= \frac{1}{\mathbf{Q}_{ii}} - 1 \\ &= \mathbf{h}_i^H (\boldsymbol{\Sigma}^{-1} + \mathbf{H}_i \mathbf{H}_i^H)^{-1} \mathbf{h}_i \end{aligned} \quad (11)$$

where  $\mathbf{h}_i$  denotes the  $i$ -th column of  $\mathbf{H}$  and  $\mathbf{H}_i$  is the result of removing the  $i$ -th column from  $\mathbf{H}$ . Note that the well-known last equality can be obtained, after some derivations, from the identity

$$[\mathbf{B}^{-1}]_{11} = \frac{1}{\mathbf{B}_{11} - \mathbf{u}_1 \mathbf{B}_1^{-1} \mathbf{v}_1} \quad (12)$$

where  $\mathbf{B}$  is a matrix of the form

$$\mathbf{B} = \begin{pmatrix} \mathbf{B}_{11} & \mathbf{u} \\ \mathbf{v} & \mathbf{B}_1 \end{pmatrix}. \quad (13)$$

Before going further, let us make a useful simplification: from now on, we will assume that  $\mathbb{E}[\mathbf{nn}^H] = N_0 \mathbf{I}$ . This assumption comes without loss of generality since, in any case,  $\boldsymbol{\Sigma}$  is positive semidefinite by definition, and therefore admits a factorization of the form  $\boldsymbol{\Sigma} = \boldsymbol{\Sigma}^{\frac{1}{2}} \boldsymbol{\Sigma}^{\frac{H}{2}}$ , so that all the results that will be derived from now on could be straightforwardly extended by simply substituting  $\mathbf{G}$  by  $\boldsymbol{\Sigma}^{-\frac{1}{2}} \mathbf{G}$ .

### III. CHARACTERIZATION OF MEAN SQUARED ERROR AND INDIVIDUAL SINR

In this section, we will start by characterizing the MSE and, from its expression, we will obtain the SINR of a given user. In order to accomplish this task, we will make a high SNR analysis.

In the high SNR regime, the LMMSE receiver converges to the Zero Forcing (ZF) receiver; recalling Equation (10), the expression of the MSE can be approximated by

$$\epsilon^2 \approx \frac{1}{K} \text{trace} \left( \frac{1}{N_0} \mathbf{H}^H \boldsymbol{\Sigma}^{-1} \mathbf{H} \right)^{-1}. \quad (14)$$

From the assumption above, and plugging the expression of  $\mathbf{H}$  from Equation (2), the result is

$$\begin{aligned} \epsilon^2 &= \frac{1}{K} \text{trace} \left( \frac{P}{N_0} \mathbf{A}^H \mathbf{G}^H \mathbf{G} \mathbf{A} \right)^{-1} \\ &= \frac{1}{K} \cdot \frac{N_0}{P} \text{trace} (\mathbf{A}^{-1} (\mathbf{G}^H \mathbf{G})^{-1} \mathbf{A}^{-H}) \\ &= \frac{1}{K} \cdot \frac{N_0}{P} \text{trace} (\mathbf{L}^{-2} (\mathbf{G}^H \mathbf{G})^{-1}). \end{aligned} \quad (15)$$

Now, in the absence of rain fading, the mean squared error would read as

$$\epsilon_u^2 = \frac{1}{K} \cdot \frac{N_0}{P} \text{trace} ((\mathbf{G}^H \mathbf{G})^{-1}) = \frac{1}{K} \frac{N_0}{P} \sum_{i=1}^K (\mathbf{G}^H \mathbf{G})_{ii}^{-1} \quad (16)$$

while the rain attenuation changes this expression to

$$\epsilon^2 = \frac{1}{K} \cdot \frac{N_0}{P} \sum_{i=1}^K l_i^{-2} (\mathbf{G}^H \mathbf{G})_{ii}^{-1} \quad (17)$$

which is, in principle, a random variable provided that the values  $l_i$  are random. In general, the pdf of  $\epsilon^2$  cannot be computed in closed form. However, its mean value can be obtained by

$$\mathbb{E}[\epsilon^2] = \frac{1}{K} \cdot \frac{N_0}{P} \sum_{i=1}^K \tilde{\mu}_i m_i \quad (18)$$

upon the assumption of independence among the different rain attenuation coefficients, and where  $\tilde{\mu}_i = \mathbb{E}[l_i^{-2}]$ . Moreover, if all the coefficients share the same mean, then the result simplifies to

$$\mathbb{E}[\epsilon^2] = \tilde{\mu} \epsilon_u^2. \quad (19)$$

In other words, the existence of rain fading scales the system mean squared error by a factor  $\tilde{\mu}$ .

The same formulation can be used to obtain the SINR experienced by a single user after LMMSE combining at the receiver. From (11), substitution yields

$$\rho_i = \frac{1}{\epsilon_i^2} - 1 = \frac{1}{l_i^{-2} \epsilon_{ui}^2} - 1 = l_i^2 (\rho_{ui} + 1) - 1, \quad (20)$$

where  $\rho_{ui}$  represents the deterministic post-combining SINR of the  $i$ -th user without rain.

In order to analyze this expression, we will need the *probability density function* (pdf) of  $l_i^2$ . To do this, we will make use of the following, more general result:

Let  $d_i = 10^{\alpha L_i}$ ,  $\alpha < 0$ , then the pdf of  $d_i$  is (see Appendix A)

$$f_d(d_i) = -\frac{1}{\sqrt{2\pi\sigma}} \cdot \frac{1}{d_i \ln d_i} \cdot e^{-\frac{1}{2} \frac{(\ln(\alpha^{-1} \ln d_i) - \beta)^2}{\sigma^2}} \quad (21)$$

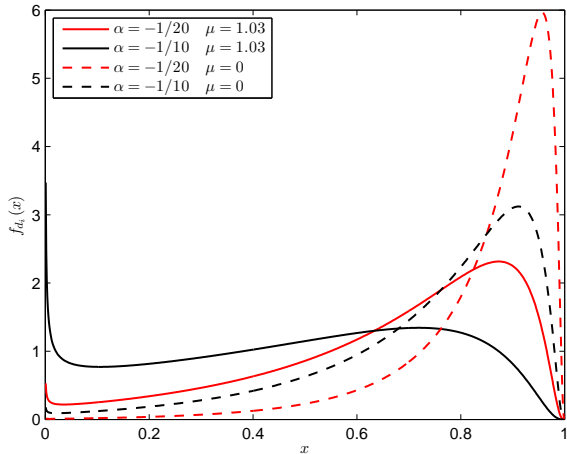


Figure 2. Probability density function of the random variable  $d_i = 10^{\alpha L_i}$  for different values of  $\alpha$  and  $\mu$ , for fixed  $\sigma = 1$ .

with  $\beta = \mu + \ln \ln 10$ ,  $d_i \in (0, 1)$  and  $\mu$  and  $\sigma$  denoting the log-normal parameters introduced in Section II-A2. For illustration purposes, Fig.2 plots the pdf for different values of the log-normal parameters and  $\alpha$ .

Coming back to our problem, setting  $\alpha = -1/10$  yields the pdf of  $l_i^2$ . Now the effect of rain fading at high SINR can be roughly seen as a scaling by a random variable in the range  $(0, 1)$  whose mean and variance lack of closed-form expressions but can be computed numerically. Note that the SINR does not depend on the rain fading experienced by other users; this is so because at high SNR the LMMSE receiver, like the ZF receiver, tends to cancel all the interference.

#### IV. CHARACTERIZATION OF THE SUM RATE

In this section, we will present the statistical characterization of the sum rate and of the *instantaneous capacity*  $\tilde{C}$ , i.e., the value of the maximum sum rate before performing the expectation. For this purpose, approximations for low and high SNR will be made, assuming perfect CSI at the receiver. While the former will be shown to share interesting symmetries with the MSE at high SNR, the latter will prove much more useful from an engineering point of view, since it will allow to compute in closed form the performance loss induced by the rain only from its statistical parameters.

##### A. High SNR

Firstly, let us rewrite the instantaneous capacity in the following way,

$$\begin{aligned} \tilde{C} &= \log_2 \det \left( \mathbf{I} + \frac{1}{N_0} \mathbf{H}^H \mathbf{H} \right) \\ &= \log_2 \det \left( \mathbf{I} + \frac{P}{N_0} \mathbf{A}^H \mathbf{G}^H \mathbf{G} \mathbf{A} \right) \\ &= \log_2 \det \left( \mathbf{I} + \frac{P}{N_0} \mathbf{L}^2 \mathbf{G}^H \mathbf{G} \right) \end{aligned} \quad (22)$$

by using the well-known identity  $\det(\mathbf{I} + \mathbf{BC}) = \det(\mathbf{I} + \mathbf{CB})$  [12]. Now, if the SNR is high, then we can approximate

$$\begin{aligned} \tilde{C}_h &\approx \log_2 \det \left( \frac{P}{N_0} \mathbf{L}^2 (\mathbf{G}^H \mathbf{G}) \right) \\ &= \log_2 \det \left( \frac{P}{N_0} \mathbf{G}^H \mathbf{G} \right) + \log_2 \det(\mathbf{L}^2) \\ &= C_{hu} - \left( - \sum_{i=1}^K 2 \log_2 l_i \right) \\ &= C_{hu} - \Delta_c \end{aligned} \quad (23)$$

where  $C_{hu}$  stands for the sum rate without rain –which is assumed deterministic– and  $\Delta_c$  is a random variable which denotes the detriment in capacity caused by rain fading. If we denote  $\xi_i = -2 \log_2 l_i$ , and recalling that  $l_i = 10^{-\frac{L_i}{20}}$ , then we have for the probability distribution of

$$\begin{aligned} \xi_i &= -2 \log_2 10^{-\frac{L_i}{20}} \\ &= \frac{1}{10 \log_{10} 2} L_i \\ &\approx \frac{1}{3} L_i, \end{aligned} \quad (24)$$

so that

$$\xi_i \sim \mathcal{LN} \left( \mu_i + \ln \left( \frac{1}{3} \right), \sigma_i^2 \right), \quad (25)$$

finally yielding

$$\Delta_c = \sum_{i=1}^K \xi_i \quad \xi \sim \mathcal{LN}(\mu_i - \ln(3), \sigma_i^2). \quad (26)$$

Unfortunately, the distribution of a sum of independent log-normal random variables does not have a closed-form expression. There are, however, a couple of alternatives that we can follow in order to complete the characterization of  $\Delta_c$ . Firstly, a log-normal approximation for the distribution of the sum was derived in [13] by matching the first and second order moments. Following this result, we would obtain

$$\begin{aligned} \Delta_c &\sim \mathcal{LN}(\mu_T, \sigma_T^2), \\ \sigma_T^2 &= \ln \left( \frac{\sum_{j=1}^K e^{2\mu_j + \sigma_j^2} (e^{\sigma_j^2} - 1)}{(\sum_{j=1}^K e^{\mu_j + \sigma_j^2/2})^2} + 1 \right), \\ \mu_T &= \ln \left( \sum_{j=1}^K e^{\mu_j + \sigma_j^2/2} \right) - \frac{\sigma_T^2}{2}. \end{aligned} \quad (27)$$

This approximation, however, results in almost intractable expressions which provide limited insight on the behavior of the term  $\Delta_c$ . In order to obtain simpler expressions, we will now make use of the assumption of  $K$  being relatively large; in this case, we can resort to the Central Limit Theorem (CLT) to obtain

$$\Delta_c \sim \mathcal{N} \left( \frac{1}{3} \sum_{i=1}^K e^{\mu_i + \sigma_i^2/2}, \frac{1}{9} \sum_{i=1}^K (e^{\sigma_i^2} - 1) e^{2\mu_i + \sigma_i^2} \right). \quad (28)$$

See Appendix B for a complete proof.

This new formulation is of great practical interest. Its most immediate application is the computation of the outage capacity, namely

$$\begin{aligned} P_{out}(C) &= \mathbb{P}[C < C_{TH}] \\ &= \mathbb{P}[\Lambda_c > C_{hu} - C_{TH}] \\ &= Q\left(\frac{C_{hu} - C_{TH} - \frac{1}{3}\sum_{i=1}^K e^{\mu_i + \sigma_i^2/2}}{\frac{1}{3}\sqrt{\sum_{i=1}^K (e^{\sigma_i^2} - 1) e^{2\mu_i + \sigma_i^2}}}\right). \end{aligned} \quad (29)$$

Another important use is the computation of the maximum sum rate, i.e.,

$$\begin{aligned} C &= \mathbb{E}[\tilde{C}] \\ &= C_{hu} - \mathbb{E}[\Delta_c] \\ &= C_{hu} - \frac{1}{3}\sum_{i=1}^K e^{\mu_i + \sigma_i^2/2}. \end{aligned} \quad (30)$$

From an engineering point of view, this result is rather interesting. It implies that, as the SNR rises, the effect of rain attenuation upon the maximum sum rate of such a multibeam satellite system is that of a constant loss in natural units, whose expression can be conveniently computed in closed form. In other words, the maximum achievable sum rate will increase as the SNR increases –since that will be the behavior of  $C_{hu}$ – and the loss induced by the rain will always be the same and, more importantly, its value can be determined in closed form from the statistical parameters of the log-normal distributions.

### B. Low SNR

To find an approximation for the low SNR regime, we will make use of the common approximation  $\ln(1+x) \approx x$ . Starting from (22), if we denote by  $\lambda_i\{\mathbf{P}\}$  the  $i$ -th largest eigenvalue of matrix  $\mathbf{P}$ , we obtain

$$\begin{aligned} \tilde{C} &= \sum_{i=1}^K \log_2\left(1 + \frac{P}{N_0}\lambda_i\{\mathbf{L}^2\mathbf{G}^H\mathbf{G}\}\right) \\ &\approx \frac{1}{\ln 2}\sum_{i=1}^K \frac{P}{N_0}\lambda_i\{\mathbf{L}^2\mathbf{G}^H\mathbf{G}\} \\ &= \frac{P}{N_0 \ln 2} \text{trace}(\mathbf{L}^2\mathbf{G}^H\mathbf{G}) \\ &= \frac{P}{N_0 \ln 2} \sum_{i=1}^K l_i^2 \|\mathbf{g}_i\|^2. \end{aligned} \quad (31)$$

It is worth noticing the similarities between the instantaneous capacity at low SNR and the MSE at high SNR; indeed, in the case where all the pdfs share the same parameters, the maximum sum rate is

$$C_l \approx \mathbb{E}\{l^2\}C_{lu} \quad (32)$$

where this time the sum rate without rain is denoted by  $C_{lu}$ . As we can see, the maximum sum rate is scaled by a factor between zero and one, depending only on the rain statistics; its value can be computed via numerical integration as will be shown in the next section.

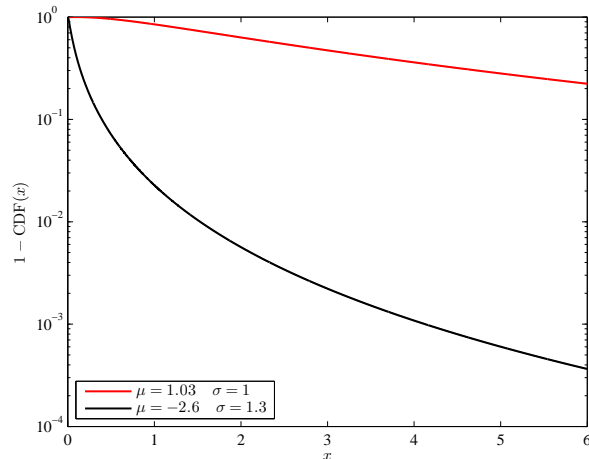


Figure 3. 1-CDF of the considered rain attenuation distributions.

## V. SIMULATION RESULTS

### A. Scenario Description

In order to test the validity of the above derived approximations, Monte Carlo simulations have been carried out for a scenario inspired on practical data. This section reports the obtained results, showing the accuracy of the expressions derived and their ranges of applicability.

The simulated scenario, for which some parameters are summarized in Table I, features  $K = 100$  beams covering the whole Europe area; the satellite antenna pattern was provided by ESA, and corresponds to an array fed reflector antenna with  $N = 155$  feeds. The user link operates at 30 GHz (Ka-band) and has a total available bandwidth of 500 MHz with full frequency reuse among the beams. Each user, however, is served by a single carrier with baudrate equal to 4 Msymb/s and guard bands that amount to the 11% of its bandwidth [14]. Users employ ACM based on the specifications given by the DVB-RCS2 standard [15].

Results have been averaged for a total of 1,000 rain fading realizations. The 100 beams have been split in halves between two possible rain fading profiles, one featuring  $(\mu = -2.6, \sigma = 1.3)$  and the other  $(\mu = 1.03, \sigma = 1)$ ; 50 beams were assigned to each profile. The former was obtained by fitting to the empirical data reported in [16], which corresponds to the city of Rome; on the other hand, the latter has been designed so as to produce an average rain attenuation of 4.6 dB, thus allowing to simulate a more rainy environment. Fig. 3 shows one minus the cumulative distribution function of each of these log-normal attenuation profiles.

A wide range of transmit powers has been covered for illustration purposes, although it is worth stressing that the most extreme values do not correspond to practical cases. Also note that, for the remainder of the paper, the term Equivalent Isotropic Radiated Power (EIRP) will refer to the EIRP per carrier.

Table I  
SIMULATION PARAMETERS

Simulation parameters	
Atmospheric fading	$(\mu = -2.6, \sigma = 1.3)$ $(\mu = 1.03, \sigma = 1)$
UTs location distribution	Fixed, one per beam
Feed gain patterns	Provided by ESA
Level of CSI	Perfect CSI
Receiver noise figure	2.5 dB
Total receiver noise temperature	517 K

### B. Results

Fig. 4 depicts the evolution of the SINR of a single user, picked at random, as a function of the EIRP per carrier. The figure shows how the derived approximation fits well above 35 dB of transmit power. As previously stated, the value of  $\mathbb{E}[I_i^2]$  seems to lack of a closed form expression, but it can be readily computed via numerical integration. The result obtained for this case was close to -3 dB which, as expected, is the separation between both curves –in the y axis– for high values of EIRP. Note that the derived approximation is intended for high SNR only, although it holds here for most of the power range because the interferers to the selected user share the same rain statistics parameters.

On the other hand, Fig. 5 shows the evolution of the maximum sum rate. For this case, approximations for both high and low SNR regimes are available, fitting rather well below 20 dBW and above 40 dBW, respectively; it is worth noticing that 42 dBW to 50 dBW is the range of EIRP values considered in the DVB-RCS implementation guidelines [17]; for comparison purposes, the figure also plots the performance results obtained by the described system when employing the DVB-RCS2 modulation and coding specifications. Again, the computation of the approximation at low SNR requires numerical integration to find  $\mathbb{E}[I_i^2]$ , while a closed form expression is available for the high SNR interval; let us remark that, although the curves with and without rain fading seem to converge, there always exists a detriment in capacity, which is additive in natural units and obeys to Equation (30). From this equation, the performance of the system above EIRP = 40 dBW can be accurately predicted from the deterministic value of  $C_{hu}$  and the rain statistics, as shown in the figure.

The behavior of the detriment in capacity is also exemplified in Fig. 6 by means of the probability of exceedance, that is, the probability of the detriment  $\Delta_c$  exceeding a certain value, shown in the x axis. Although the accuracy does not seem remarkable, it does provide information about the system's behavior by taking into account only the statistics of the rain fading.

## VI. CONCLUSIONS

In this paper, we have obtained expressions for the SINR and maximum sum rate of a multibeam satellite system that performs LMMSE interference canceling but suffers from rain

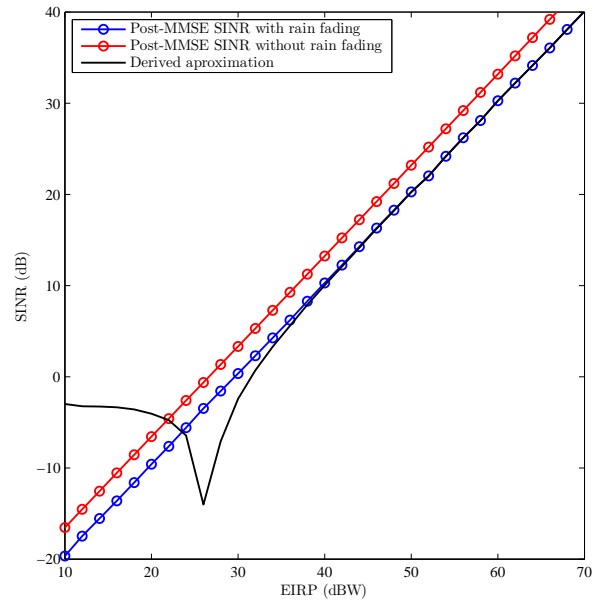


Figure 4. Post-MMSE combining SINR of a user, chosen at random. Half of the users experiment ( $\mu_i = 1.03, \sigma_i = 1$ ) and the other half ( $\mu_i = -2.6, \sigma_i = 1.3$ ).

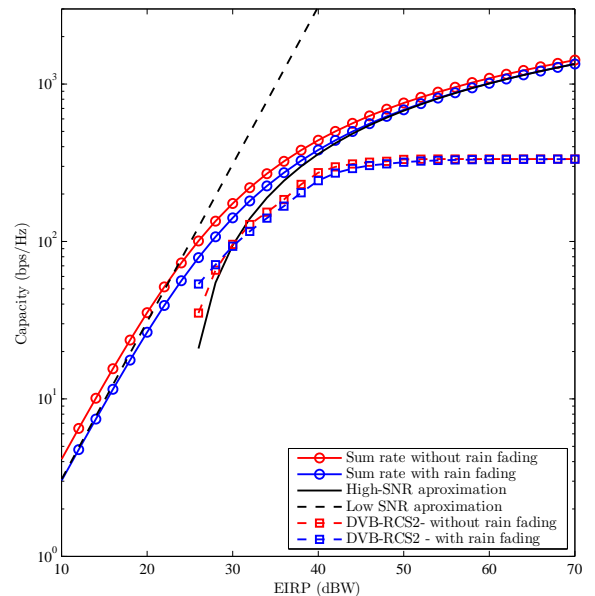


Figure 5. Evolution of the sum rate as a function of the EIRP per carrier. Half of the users experiment ( $\mu_i = 1.03, \sigma_i = 1$ ) and the other half ( $\mu_i = -2.6, \sigma_i = 1.3$ ).

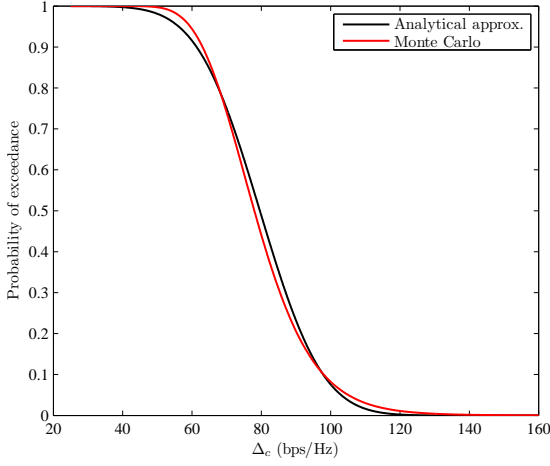


Figure 6. Probability of the detriment in capacity exceeding some value. Half of the users experiment ( $\mu_i = 1.03$ ,  $\sigma_i = 1$ ) and the other half ( $\mu_i = -2.6$ ,  $\sigma_i = 1.3$ ).

attenuation. It has been shown that, as the SNR grows, the loss in terms of sum rate tends to be a constant value depending only on the statistics of the rain fading processes, while a user's SINR tends to suffer a scaling which depends on its rain attenuation only. Computer simulations have demonstrated the accuracy of the derived expressions, illustrating also other relevant issues such as the probability of outage and the performance gap with respect to a system employing DVB-RCS2.

#### APPENDIX A

##### DERIVATION OF THE PDF OF $10^{\alpha L_i}$

As already stated, the rain attenuation in dB follows a log-normal distribution, but in this work we will be more interested in modeling it in natural units, though, since this is the value that appears in matrix  $\mathbf{L}$ . Its expression will be given by  $l_i = 10^{-\frac{L_i}{20}}$  where we are assuming that  $L_i$  is a value to be subtracted in dB, and therefore the minus sign in the exponent is necessary. However, through this work we will need to characterize the pdf not only of the attenuation, but also of its value squared. For this reason, we will state the more general problem of deriving the pdf of  $d_i = 10^{\alpha L_i}$ , with  $\alpha < 0$ , and we will change  $\alpha$  according to our needs.

This is nothing but the problem of deriving the pdf of a random variable transformation, which can be written as

$$d_i = g(L_i) = 10^{\alpha L_i}. \quad (33)$$

According to [18], the pdf of a transformation follows

$$f_d(d_i) = f_L(g^{-1}(d_i)) \left| \frac{\partial g^{-1}(d_i)}{\partial d_i} \right|. \quad (34)$$

From this expression, differentiation and substitution yields

$$g^{-1}(d_i) = \frac{\ln d_i}{\alpha \ln 10} \quad (35)$$

$$\left| \frac{\partial g^{-1}(d_i)}{\partial d_i} \right| = \frac{1}{|\alpha| d_i \ln 10}$$

where we have used the fact that  $d_i$  will always be positive. Now, recalling that

$$f_L(L_i) = \frac{1}{L_i \sqrt{2\pi\sigma}} \cdot e^{-\frac{1}{2} \frac{(\ln L_i - \mu)^2}{\sigma^2}}, \quad (36)$$

we can substitute to obtain

$$f_d(d_i) = \frac{1}{d_i |\alpha| \ln 10} \frac{1}{\frac{\ln d_i}{\alpha \ln 10} \sqrt{2\pi\sigma}} e^{-\frac{1}{2} \frac{(\ln(\alpha^{-1} \ln d_i) - \ln \ln 10 - \mu)^2}{\sigma^2}}$$

$$= -\frac{1}{\sqrt{2\pi\sigma}} \cdot \frac{1}{d_i \ln d_i} \cdot e^{-\frac{1}{2} \frac{(\ln(\alpha^{-1} \ln d_i) - \beta)^2}{\sigma^2}} \quad (37)$$

with

$$\beta = \mu + \ln \ln 10. \quad (38)$$

In what refers to the *cumulative distribution function* (cdf), its expression is obtained by integration and results into

$$F_d(d_i) = -\frac{1}{2} \left( -2 + \operatorname{erfc} \left( \frac{-\ln(\alpha^{-1} \ln d_i) + \beta}{\sqrt{2}\sigma} \right) \right) \quad (39)$$

$$= Q \left( \frac{\ln(\alpha^{-1} \ln d_i) - \beta}{\sigma} \right).$$

#### APPENDIX B

##### PROOF OF EQUATION (28)

First of all, we must prove that the CLT can be applied in this case, even though the random variables are not i.i.d. The following is known to be a set of sufficient conditions for the CLT to hold (see [18, p. 283]):

- 1) The sum of the variances tends to infinity as the number of variables increases:

$$\lim_{n \rightarrow \infty} \sum_{i=1}^n \sigma_i^2 = \infty. \quad (40)$$

- 2) There exist some  $c > 2$  and some finite  $K$  such that

$$\int x^c f_i(x) dx < K \quad \forall i. \quad (41)$$

The first proposition is trivial to prove in our case, since  $\sigma_i^2 > 0 \forall i$ . With respect to the second proposition, we need to prove that some central moment of order higher than two is finite for all the involved variables. To do so, we will first obtain the expression of any central moment as [19]

$$m_\xi(c) = \int x^c f_\xi(x) dx = \frac{1}{3} e^{c\mu + \sigma^2 c^2 / 2}. \quad (42)$$

From this expression, it is clear that the second condition also holds and, as a consequence, the CLT can be applied. The expression of  $\Delta_c$  would then be

$$\Delta_c \sim \mathcal{N} \left( \sum_{i=1}^K \hat{\mu}_i, \sum_{i=1}^K \hat{\sigma}_i^2 \right) \quad (43)$$

where  $\hat{\mu}_i$  and  $\hat{\sigma}_i^2$  stand for the mean and variance of the  $i$ -th log-normal component, respectively (note that the ordinary log-normal distribution parameters  $\mu$  and  $\sigma^2$  represent different things, namely, the *location parameter* and the *scale parameter*), and their expressions follow

$$\hat{\mu}_i = m_\xi(1) = \frac{1}{3} e^{\mu + \sigma^2/2} \quad (44)$$

and

$$\begin{aligned} \hat{\sigma}_i^2 &= \int (x - \hat{\mu}_i)^2 f_\xi(x) dx \\ &= \frac{1}{9} \left( e^{\sigma_i^2} - 1 \right) e^{2\mu_i + \sigma_i^2}, \end{aligned} \quad (45)$$

thus concluding the proof.

It is important to notice that the probability of  $\Delta_c$  being negative, i.e.,

$$P[\Lambda_c < 0] = 1 - Q \left( - \frac{\sum_{i=1}^K e^{\mu_i + \sigma_i^2/2}}{\sqrt{\sum_{i=1}^K (e^{\sigma_i^2} - 1) e^{2\mu_i + \sigma_i^2}}} \right) \quad (46)$$

is negligible because, in general, the argument of the  $Q$  function will be a large negative number, thus rendering  $Q \approx 1$  and  $P[\Lambda_c < 0] \approx 0$ . This is consequent with its physical meaning, since rain attenuation cannot cause an increase in the performance of the system.

#### REFERENCES

- [1] G. Caire, M. Debbah, L. Cottatellucci, R. De Gaudenzi, R. Rinaldo, R. Mueller, and G. Gallinaro, "Perspectives of adopting interference mitigation techniques in the context of broadband multimedia satellite systems," in *ICSSC 2005, 23rd AIAA International Communications Satellite Systems Conference, 25-28 September, 2005, Rome, Italy*, 09 2005.
- [2] L. Cottatellucci *et al.*, "Interference mitigation techniques for broadband satellite systems," in *Proc. 24th AIAA Int. Commun. Satell. Systems Conf., ICSSC*, Jun. 2006.
- [3] J. Arnau-Yanez, M. Bergmann, E. Candreva, G. Corazza, R. de Gaudenzi, B. Devillers, W. Gappmair, F. Lombardo, C. Mosquera, A. Perez-Neira, I. Thibault, and A. Vanelli-Coralli, "Hybrid space-ground processing for high-capacity multi-beam satellite systems," in *Global Telecommunications Conference (GLOBECOM 2011), 2011 IEEE*, dec. 2011, pp. 1–6.
- [4] G. Gallinaro, M. Debbah, R. Müller, R. Rinaldo, and A. Vernucci, "Interference Mitigation for the Reverse-Link of Interactive Satellite Networks," in *9th International Workshop on Signal Processing for Space Communications*, Sep. 2006.
- [5] O. Somekh and S. Shamai, "Shannon-theoretic approach to a gaussian cellular multiple-access channel with fading," *Information Theory, IEEE Transactions on*, vol. 46, no. 4, pp. 1401–1425, jul 2000.
- [6] D. Tse and P. Viswanath, *Fundamentals of wireless communication*. New York, NY, USA: Cambridge University Press, 2005.
- [7] J. Choi, *Optimal Combining and Detection: Statistical Signal Processing for Communications*, 1st ed. New York, NY, USA: Cambridge University Press, 2010.
- [8] A. Paulraj, R. Nabar, and D. Gore, *Introduction to Space-Time Wireless Communications*, 1st ed. New York, NY, USA: Cambridge University Press, 2008.
- [9] S. Chatzinotas, G. Zheng, and B. Ottersten, "Joint precoding with flexible power constraints in multibeam satellite systems," in *Global Telecommunications Conference (GLOBECOM 2011), 2011 IEEE*, dec. 2011, pp. 1–5.
- [10] J. Arnau, B. Devillers, C. Mosquera, and A. Perez-Neira, "Performance study of multiuser interference mitigation schemes for hybrid broadband multibeam satellite architectures," *EURASIP Journal on Wireless Communications and Networking*, vol. 2012, no. 1, p. 132, 2012. [Online]. Available: <http://jwcn.eurasipjournals.com/content/2012/1/132>
- [11] I. E. Telatar, "Capacity of multi-antenna gaussian channels," *EUROPEAN TRANSACTIONS ON TELECOMMUNICATIONS*, vol. 10, pp. 585–595, 1999.
- [12] G. H. Golub and C. F. Van Loan, *Matrix Computations (Johns Hopkins Studies in Mathematical Sciences)*, 3rd ed. The Johns Hopkins University Press, Oct. 1996.
- [13] L. Fenton, "The sum of log-normal probability distributions in scatter transmission systems," *Communications Systems, IRE Transactions on*, vol. 8, no. 1, pp. 57–67, march 1960.
- [14] H. Brandt, O. Lücke, V. Boussemart, C. Párraga-Niebla, T. Flo, C. Kissling, and R. Schweikert, "Resources Management using Adaptive Fade Mitigation Techniques in DVB-S2/RCS Multi-Beam Systems," in *Proceedings of the 25th International Communications Satellite Systems Conference (ICSSC 2007)*, 2007.
- [15] ETSI, "Digital Video Broadcasting (DVB); Second Generation DVB Interactive Satellite System; Part 2: Lower Layers for Satellite standard," March 2011.
- [16] N. Zorba, M. Realp, and A. Perez-Neira, "An improved partial CSIT random beamforming for multibeam satellite systems," in *Signal Processing for Space Communications, 2008. SPSC 2008. 10th International Workshop on*, oct. 2008, pp. 1–8.
- [17] ETSI, "Digital Video Broadcasting (DVB); Interaction channel for Satellite Distribution Systems; Guidelines for the use of EN 301 790," July 2009.
- [18] A. Papoulis and S. Pillai, *Probability, random variables, and stochastic processes*, 4th ed. McGraw-Hill, 2002.
- [19] M. K. Simon, *Probability Distributions Involving Gaussian Random Variables: A Handbook for Engineers, Scientists and Mathematicians*. Secaucus, NJ, USA: Springer-Verlag New York, Inc., 2006.